NASA TECHNICAL MEMORANDUM

NASA TM X-1991

NASA TM X-1991

DESIGN AND TWO-DIMENSIONAL CASCADE TEST OF TURBINE STATOR BLADE WITH RATIO OF AXIAL CHORD TO SPACING OF 0.5

by Roy G. Stabe

Lewis Research Center

Cleveland, Ohio

NATIONAL AERONAUTICS AND SPACE ADMINISTRATION • WASHINGTON, D. C. • APRIL 1970

1. Report No. NASA TM X-1991	2. Government Accession No.	3. Recipient's Catalog No.
4. Title and Subtitle DESIGN AND TWO-DIMENSIONAL CASCADE TEST OF TURBINE STATOR BLADE WITH RATIO OF AXIAL CHORD TO SPACING OF 0.5		5. Report Date April 1970 6. Performing Organization Code
7. Author(s) Roy G. Stabe		8. Performing Organization Report No. E-5490
9. Performing Organization Name and Address Lewis Research Center National Aeronautics and Space Administration Cleveland, Ohio 44135		10. Work Unit No. 720-03 11. Contract or Grant No. 13. Type of Report and Period Covered Technical Memorandum
12. Sponsoring Agency Name and Address National Aeronautics and Space Administration Washington, D.C. 20546		14. Sponsoring Agency Code
15. Supplementary Notes		

16. Abstract

Blades were designed for a velocity diagram typical of the first-stage stator of a jet engine turbine and were tested in a simple two-dimensional cascade of six blades. The principal measurements were blade surface static pressure and cross-channel surveys of exit total pressure, static pressure, and flow angle. The results of the experimental investigation include blade loading in terms of the blade surface pressures and overall performance in terms of the loss and blade loading coefficients. Also included is a comparison of the experimentally and analytically obtained blade surface velocity distribution and the cross-channel variation of velocity and flow angle.

17. Key Words (Suggested by Author(s))	18. Distribution Statement
Turbine blades Low solidity Design Performance	Unclassified - unlimited

19. Security Classif. (of this report)	20. Security Classif. (of this page)	21. No. of Pages	22. Price*
Unclassified	Unclassified	21	$3.00

*For sale by the Clearinghouse for Federal Scientific and Technical Information
Springfield, Virginia 22151

DESIGN AND TWO-DIMENSIONAL CASCADE TEST OF TURBINE STATOR BLADE WITH RATIO OF AXIAL CHORD TO SPACING OF 0.5

by Roy G. Stabe

Lewis Research Center

SUMMARY

The design of very low-solidity turbine stator blades is described, and the results of an experimental investigation of the performance of these blades is presented. The blades were designed for a velocity diagram typical of the first stage of a jet engine turbine. The blade design criterion was high blade loading effectiveness. The performance of the blades was investigated experimentally in a simple two-dimensional cascade of six blades. The results of these tests are summarized as follows:

The flow apparently remained attached to the suction surfaces of the blades up to an ideal exit velocity ratio $(v/v_{cr})_{id,3}$ of about 0.7. At higher exit velocity ratios, separation began to occur. The separation and kinetic energy loss increased gradually up to an exit velocity ratio of about 0.77. At this point, separation and loss increased rapidly. At exit velocity ratios higher than 0.81, separation became severe. The rapid increase in separation and loss was correlated to the occurrence of supersonic velocities on the blade suction surfaces. The rapidly increasing separation and loss were probably influenced by shock interaction with the boundary layer.

A high blade loading effectiveness was achieved. At an exit velocity ratio of 0.75, the blade loading effectiveness was 0.715. However, a velocity peak occurred on the suction surface of the blade at about 75 percent of the axial chord. A modification of the suction surface to reduce these peak velocities would increase the blade loading effectiveness and delay the rapid increase in separation and loss to higher exit velocities.

The wide blade spacing and the high curvature and angles on the suction surface of the blade caused large variations in flow angle, static pressure, and weight flow across the channel in the plane of the trailing edge. The highest values of flow angle and static pressure and the lowest value of weight flow occurred near the suction surface of the blade.

The variation of velocity and flow angle across the channel in the plane of the trailing edge and the blade surface velocities was very close to the values predicted by a computer program similar to the one used in the design of the blades.

INTRODUCTION

The NASA Lewis Research Center is engaged in a program investigating advanced concepts to increase turbine blade loading. The use of highly loaded blading effects a reduction in turbine size and weight through the use of fewer stages, a smaller diameter, or fewer blades. The use of fewer blades in high-temperature applications also reduces the blade cooling air requirement.

As the number of blades (the solidity) decreases, the force or loading on each blade must, of course, increase. The higher loading is evidenced by higher velocity on the suction surface of the blades and also by larger deceleration or diffusion. This larger diffusion is associated with higher loss and eventual flow separation. The design of highly loaded blading thus depends on the minimization of diffusion and its effects. Stewart and Glassman (ref. 1) showed that, for a given velocity diagram, the product of solidity (based on axial chord), blade loading effectiveness, and a form of suction surface diffusion is constant. For a given velocity diagram, then, low solidities can be obtained by maximizing the product of diffusion and loading effectiveness. Although both factors are related, the two approaches suggested are directed at obtaining (a) high suction surface diffusion in conjunction with boundary layer control devices and (b) high loading effectiveness. In general, boundary layer control devices deal primarily with increasing the permissible level of diffusion prior to flow separation. References 2 to 4 are representative of studies made on two such devices, namely, tandem and jet flap blades. Efforts to reduce the solidity of plain blades, in general, deal with increasing the loading effectiveness. This report is concerned with studying the performance of a plain blade designed for a very low solidity by utilizing a high loading effectiveness.

A typical stator blade was arbitrarily selected to approximate design conditions in terms of an imposed velocity diagram. The blades selected are described by Whitney et al. (ref. 5). These blades were designed for a velocity diagram typical of the first-stage stator of a jet engine turbine and yielded an efficiency of 0.965. The solidity, based on axial chord, was 1.0 at the mean radius. This solidity is less than the optimum value obtained from such standard references as Zweifel (ref. 6) or Miser, Stewart, and Whitney (ref. 7). The solidity of the subject blade was reduced to 0.5, which is one-half that of the reference blade. For the same velocity diagram, this is equivalent to doubling the blade loading. The purpose of the program, then, is to design blades that achieve this very high loading without sacrificing the high efficiency of the reference blades.

The performance of the blades was investigated experimentally in a simple two-dimensional cascade of six blades. The principal measurements were blade surface static pressure and cross-channel surveys of exit total pressure, static pressure, and

flow angle. These data were taken at several ideal exit critical velocity ratios between 0.59 and 0.81. The results of the experimental investigation presented include the blade loading in terms of the blade surface pressures and the overall performance in terms of the loss and blade loading coefficients. Also included is a comparison of the experimentally and analytically obtained blade surface velocity distribution and the cross-channel variation of velocity and flow angle.

SYMBOLS

a	distance along axial chord from blade leading edge, in.; cm
C_a	blade axial chord, in.; cm
D_s	blade suction surface diffusion factor, $(p_1' - p_{s,min})/(p_1' - p_3)$
$\bar{e}$	kinetic energy loss coefficient, $1 - V_3^2/V_{3,id}^2$
p	absolute pressure, psi; N/cm^2
s	blade spacing or distance in tangential direction, in.; cm
v	velocity, ft/sec; cm/sec
α	flow angle, deg from axial
ρ	density, lb/ft^3; kg/cm^3
ψ	loading effectiveness parameter
ψ_Z	Zweifel loading coefficient

Subscripts:

cr	flow conditions at Mach 1
id	ideal of isentropic process
max	maximum value
min	minimum value
s	blade suction surface
1	station at blade inlet
2	station at blade exit survey plane
3	station at blade exit where flow conditions are assumed uniform

Superscript:

'	total state condition

BLADE DESIGN

The blade design was based on the stator blades described in reference 5. The reference blades were designed for velocity diagrams typical of the first-stage stator for a jet engine turbine. The subject blades were designed for a similar mean section velocity diagram and for the same axial chord and trailing edge radius as the reference blades. The solidity, based on axial chord, of the reference blades was 1.0. For the subject blades, the axial solidity was reduced to 0.5, which in effect, doubled the loading. The blades were designed for high blade loading effectiveness, which means that they were designed for high velocities over the length of the suction surface and low velocities over the length of the pressure surface. This velocity distribution minimizes as much as possible the amount of diffusion required for the imposed velocity diagram.

The blade geometry and velocity diagram are illustrated in figure 1. The blade coordinates are given in table I. As shown in figure 1, the blades are set at a large angle to the inlet flow. This high stagger results in low velocities along the pressure surface. A large, blunt leading edge was used to quickly accelerate the flow to high velocity on the suction surface. The suction surface was then successively adjusted to maintain this high velocity over most of its length.

A computer program, developed by Katsanis (ref. 8) was used to determine the blade surface velocities. This program uses a finite difference solution of the stream function equation. This method is applicable to low-solidity blading where the guided portion of the flow channel is very short. At the time the blades were being designed, the program was for incompressible flow only. The program has since been expanded and refined and can now be used for compressible flow with transonic velocities (ref. 9). Both programs are for ideal or isentropic flow.

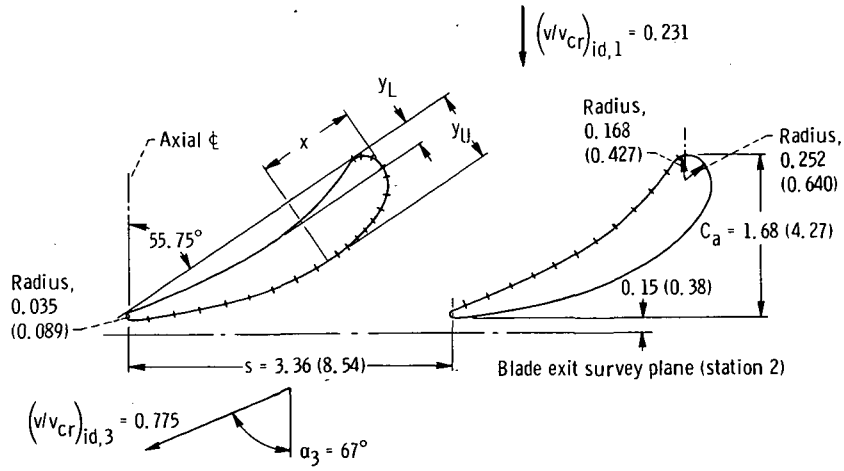

Figure 1. - Stator blade geometry. (Location of blade surface taps is indicated by hash marks on blades.) All dimensions are in inches (cm).

TABLE I. - STATOR BLADE COORDINATES

x		y_L		y_U	
in.	cm	in.	cm	in.	cm
0	0	0.237	0.602	0.237	0.602
.025	.064	-----	-----	.352	.894
.05	.127	-----	-----	.402	1.021
.1	.254	-----	-----	.467	1.186
.15	.381	-----	-----	.513	1.303
.2	.508	-----	-----	.547	1.389
.25	.635	-----	-----	.575	1.460
.3	.762	.026	.066	.598	1.519
.4	1.016	.066	.168	.633	1.608
.5	1.270	.103	.262	.660	1.676
.6	1.524	.133	.338	.680	1.727
.7	1.778	.160	.406	.692	1.758
.8	2.032	.182	.462	.700	1.778
0.9	2.285	0.200	0.508	0.705	1.791
1.0	2.540	.213	.541	.705	1.791
1.1	2.794	.223	.566	.702	1.783
1.2	3.048	.230	.584	.697	1.778
1.3	3.302	.234	.594	.687	1.745
1.4	3.556	.235	.597	.675	1.714
1.5	3.810	.234	.594	.657	1.669
1.6	4.064	.230	.584	.635	1.613
1.7	4.318	.223	.566	.612	1.554
1.8	4.572	.215	.546	.585	1.486
1.9	4.826	.205	.521	.556	1.412
2.0	5.08	.192	.488	.523	1.328
-----	-----	-----	-----	-----	-----
2.1	5.334	0.178	0.452	0.487	1.237
2.2	5.588	.162	.411	.450	1.143
2.3	5.842	.143	.363	.410	1.041
2.4	6.096	.125	.318	.370	.740
2.5	6.35	.105	.267	.327	.831
2.6	6.604	.086	.218	.282	.716
2.7	6.858	.065	.165	.234	.594
2.8	7.112	.045	.114	.184	.467
2.9	7.366	.025	.064	.134	.340
3.0	7.62	.004	.010	.084	.213
3.019	7.668	0	0	.074	.188
3.054	7.757	.035	.089	.035	.089
-----	-----	-----	-----	-----	-----

APPARATUS AND PROCEDURE

Cascade

The blades were tested in a simple two-dimensional cascade of six blades. Figure 2 shows the cascade tunnel with the adjustable inlet guide walls and the survey prove traversing mechanism. Another view of the cascade tunnel with one of the end walls removed is presented in figure 3. This figure also shows the blading and the location of the inlet and exit guide walls. The inlet guide walls were set to the approximate location of the stagnation streamlines of the end blades. The exit guide walls are about 4 inches (10.15 cm) away from the end blades. In this position, the walls do not contribute substantially to the turning of the flow. The spacing between end walls, or the blade length, was 4 inches (10.15 cm). Boundary layer suction was not used.

Surveys of total pressure at the blade exit and wall static-pressure measurements at the blade inlet and exit were used to determine the two dimensionality of the flow through the cascade. The total pressure surveys were made at several distances between the end wall and the blade midspan. These measurements indicated that the flow

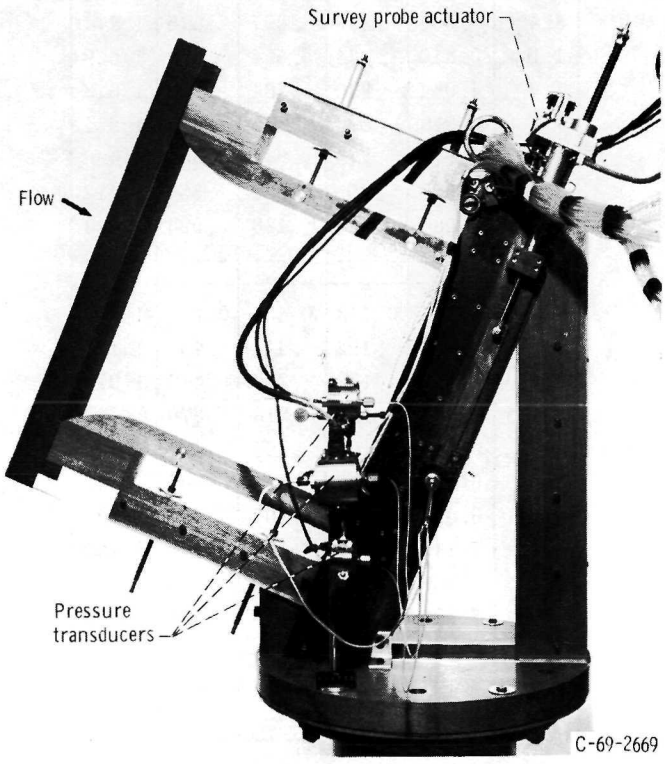

Figure 2. - Stator blade cascade.

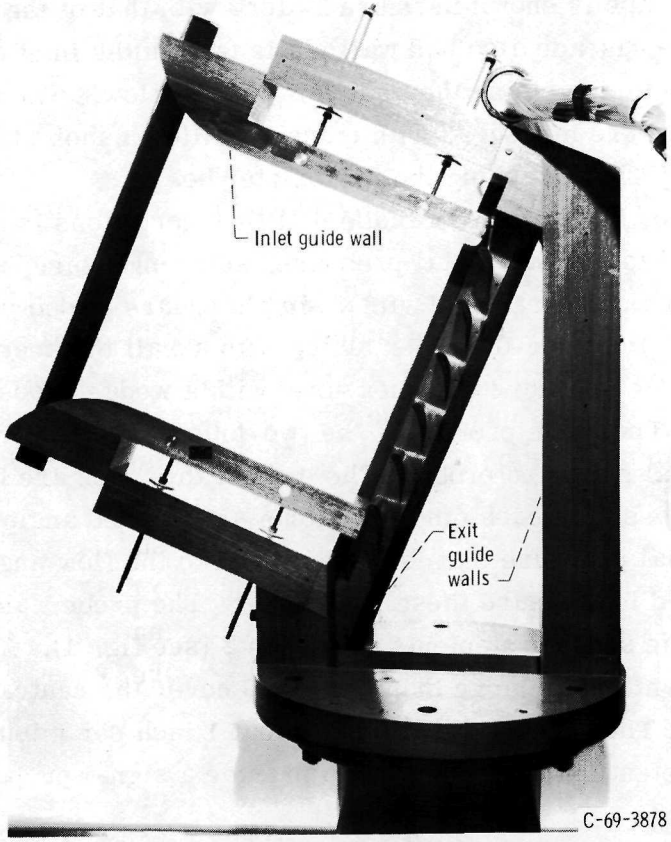

Figure 3. - Stator blade cascade showing arrangement of blades and end walls.

through the center 2 inches (5.08 cm) of the blade span was not affected by the end wall boundary layer and that the flow conditions were about the same in the center three passages of the cascade. Therefore, measurements taken at the mean section of the center channel should be representative of the blade performance.

In operation, room air was drawn through the inlet section and blading, through an exhaust control valve, and into the laboratory altitude exhaust system. The pressure ratio was maintained by regulation of the exhaust control valve. The blades were tested over a range of inlet total- to exit static-pressure ratio p_1'/p_3 of about 1.24 to 1.50. The corresponding range of exit ideal critical velocity ratios $(v/v_{cr})_{id,3}$ was 0.59 to 0.81.

Instrumentation

The two blades that formed the center channel of the cascade were instrumented at midspan with static-pressure taps. The static tap diameter was 0.020 inch (0.05 cm).

The location of these taps is shown in figure 1 along with that of the blade exit survey plane, station 2. The cascade also had wall static taps in the inlet and exit sections. These taps were used to determine the uniformity of the flow. The blade surface and wall static pressures were measured with mercury-filled manometers. The pressure data were recorded by photographing the manometer board.

The probe used for the surveys of blade exit flow conditions is shown in figure 4. The probe is equipped to measure total pressure, static pressure, and flow angle.

The total pressure was measured with a simple square-ended probe made from 0.020-inch- (0.5-mm-) outside-diameter tubing with a wall thickness of 0.0025 inch (0.062 mm). The static pressure was measured with a wedge probe that had an included angle of 15°. The angle probe was the two-tube type made from tubing the same size as that of the total pressure probe. The ends of the tubes are cut at 45° so that the leveled ends of the tubes face each other and form an included angle of 90°. The probe measures a differential pressure that is proportional to the flow angle. Strain-gage transducers were used to measure these pressures. The probe was fixed at the average exit flow angle with the sensing elements at station 2 (see fig. 1). The probe traversed 5 inches (12.7 cm), which was more than enough to cover the central channel and the two boundary wakes. The traverse speed was about 1 inch per minute (2.54 cm/min). An actuator-driven potentiometer was used to provide a signal proportional to the probe position.

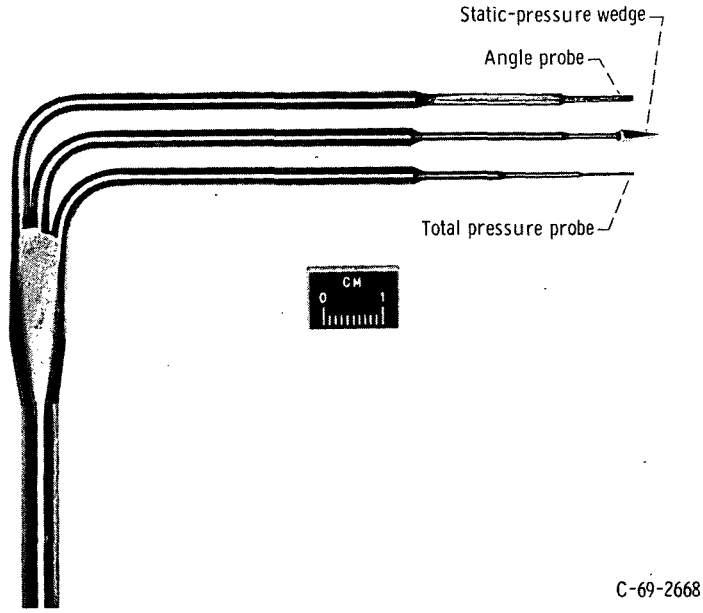

Figure 4. - Combination exit survey probe.

The output signals of the three pressure transducers were recorded as a function of probe position on x, y-recorders. The output signals of the three pressure transducers and of the probe position potentiometer were also digitalized and recorded on magnetic tape. The recording rate was 20 words per second.

Data Reduction

Blade surface static pressures were taken from the photographs of the manometer board. These data were used to calculate the blade loading parameters and blade surface velocities. A computer was used to reduce the blade exit survey data recorded on magnetic tape. The flow angle, velocity, and flow per unit area were calculated from these data as a function of probe position. The weight flow, momentum, tangential component of momentum, and flow-energy-averaged ideal velocity were computed using a Simpson's rule integration over a distance equal to one blade space. An average static pressure for station 2 (the survey plane) was calculated from the average ideal velocity. The continuity and conservation of momentum and energy relations were then used to calculate the flow angle, velocity, and pressure at a hypothetical location where flow conditions were assumed uniform. This hypothetical location is designated station 3. For these calculations, the tangential component of momentum was assumed constant between stations 2 and 3.

RESULTS AND DISCUSSION

The results of the investigation of blade performance in the two-dimensional cascade are presented in three sections: the general results from the blade exit surveys and blade surface static-pressure measurements; the overall performance in terms of the loss, diffusion, and blade loading; and a comparison of the experimentally determined blade surface velocities and the blade exit velocities and angles with the values computed using reference 9.

General

Blade exit surveys. - A typical x, y-plotter record of a blade exit survey of total and static pressure is presented in figure 5. The figure shows the wakes of the two blades bounding the center channel of the cascade and the variation of static pressure across the channel. This variation is about 2.5 psi (1.72 N/cm^2). The peak static pressure

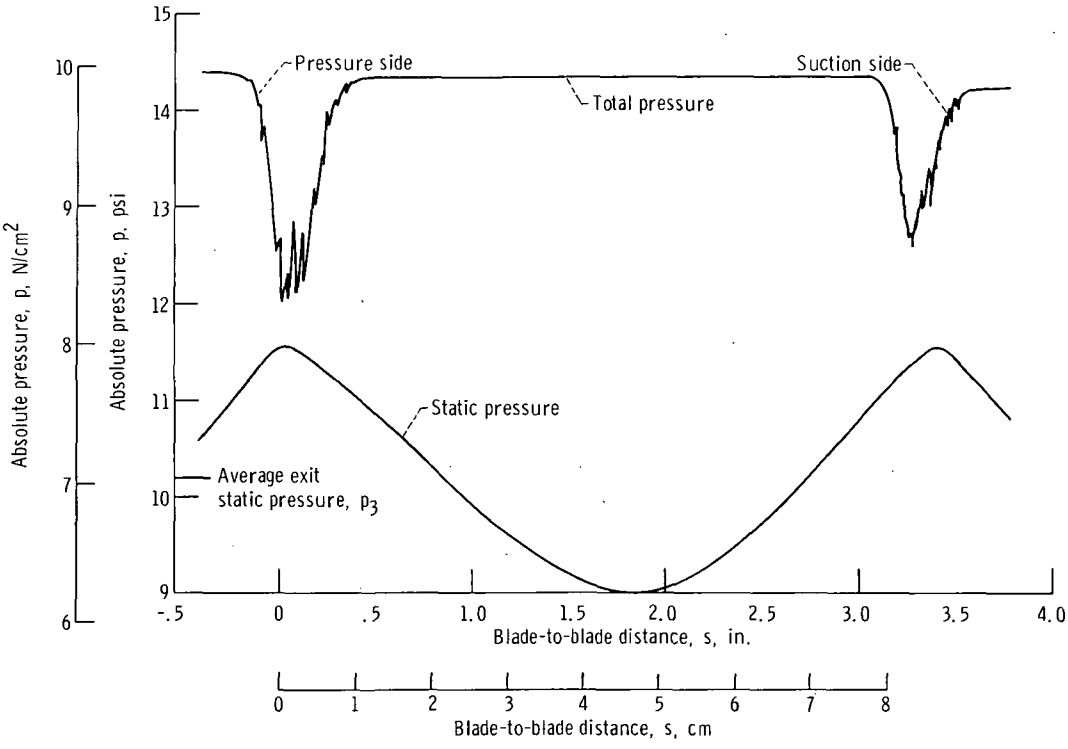

(a) Pressure.

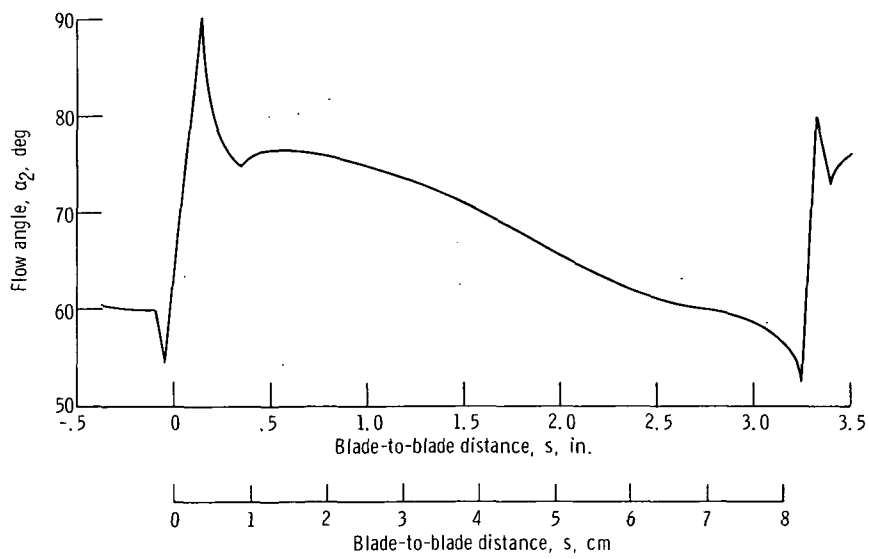

(b) Flow angle.

Figure 5. - Blade-to-blade variation of total pressure, static pressure, and flow angle at station 2. Exit survey taken at ideal exit velocity ratio of 0.75.

occurs opposite the blade trailing edges. The minimum static pressure occurs near the center of the channel. The static pressure became progressively more uniform farther downstream. At a distance of one blade chord axially downstream of the blade trailing edges, the static-pressure variation across the channel was about 0.25 psi (0.17 N/cm^2).

The total pressure trace shows some differences in the two wakes. The reason for this may be small differences in geometry or in operating characteristics. The losses were calculated for both blades and were about the same.

The variation in flow angle across the channel is shown in figure 5(b). The angle data are from the same survey as the pressure data shown in figure 5(a). The flow angle changed almost linearly from about 76° at the suction side of the wake on the left to about 56° at the pressure side of the wake on the right. This very large angle variation was not unexpected and results from the wide blade spacing in conjunction with the high curvature and large suction surface blade angles. The average flow angle calculated at station 3 was 69.2° for this survey.

The changes in the wakes as the exit velocity was increased are shown in figure 6. The width and depth of the wakes were approximately constant up to an exit velocity ratio of 0.70. As the exit velocity increased, the wakes became progressively deeper and wider on the suction surface side. The flow apparently remained attached up to an

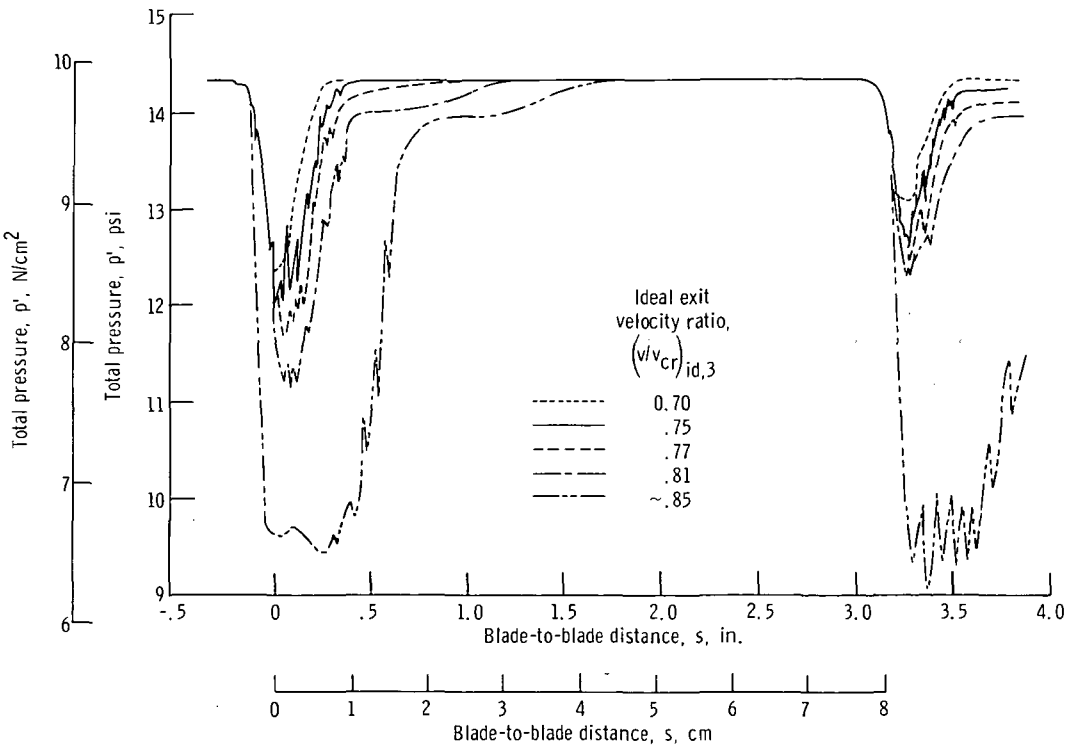

Figure 6. - Blade-to-blade variation of total pressure with exit velocity.

exit velocity ratio of about 0.7. At higher exit velocities, separation began to occur and increased gradually up to an exit velocity ratio of 0.77. At this point, the region of total pressure loss had begun to extend into the free stream. The area of this additional loss increased rapidly as the exit velocity increased. When an attempt was made to operate the cascade at exit velocity ratios higher than 0.81, separation became severe.

Weight flow. - The large blade-to-blade variations in pressure and flow angle discussed in the previous section resulted in a correspondingly large variation in weight flow across the channel. A typical distribution of flow across the channel is shown in figure 7, where the flow per unit area of the center channel is plotted against the blade-to-blade distance. There is substantially less flow in the region extending from the wake of the left blade to approximately midchannel. The flow angles in this region were very large and were the principal reason for the lower flow.

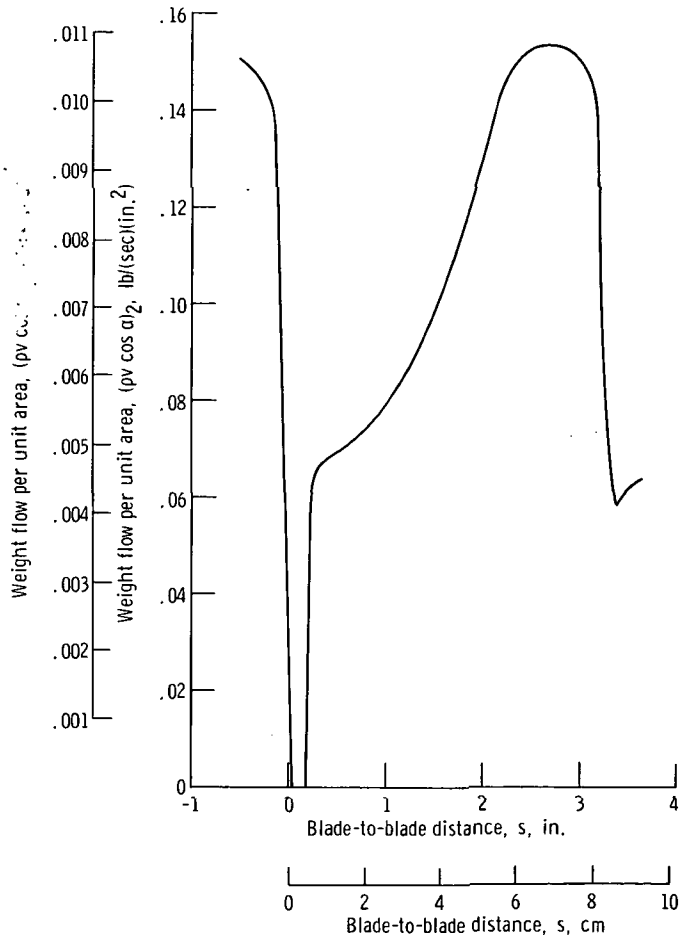

Figure 7. - Blade-to-blade variation of weight flow per unit area at station 2. Exit survey taken at ideal exit velocity ratio of 0.75.

Blade loading. - The blade loading computed from blade surface static-pressure measurements for three ideal exit velocity ratios is shown in figure 8. It is convenient to express blade loading in terms of the parameter used in this figure because the area enclosed by the curves is equal to the Zweifel loading coefficient ψ_z. In addition, the maximum value of the parameter is equal to the suction surface diffusion factor D_s. The Zweifel coefficient is defined as the ratio of the tangential component of the actual blade pressure force to an ideal force based on the difference between the inlet total and exit static pressure acting on the axial chord. The blade loading effectiveness parameter ψ is similarly defined except that the ideal force is based on the difference between the inlet total pressure and the minimum blade suction surface pressure. The two parameters are related as

$$\psi = \frac{\psi_z}{D_s}$$

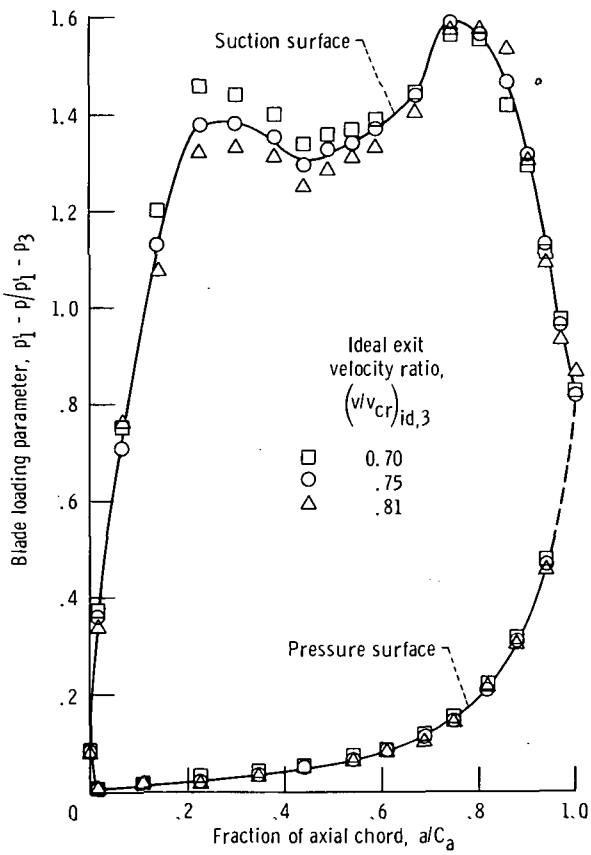

Figure 8. - Blade loading computed from blade surface static pressures.

The curves in figure 8 are drawn through the data for an ideal exit velocity ratio of 0.75. Low values of loading parameter occur over most of the pressure surface. On the suction surface, the loading parameter increases to high values close to the leading edge, remains at high values over the middle portion of the suction surface, and then decreases rapidly over the last 20 percent of axial chord. This decrease, or diffusion, extends to static pressures that are higher than the exit static pressure. This occurs because the static pressure at the trailing edge was higher than the exit static pressure p_3 (see fig. 5(a)). The actual diffusion on the suction surface of these blades is thus higher than indicated by the diffusion parameter, which is based on the exit static pressure.

For the curves shown, the Zweifel loading coefficient is 1.135 and the diffusion is 1.59, which results in a loading effectiveness of 0.715. One improvement in the design of this blade would be to modify the suction surface to eliminate the peak at 75 percent axial chord. This modification would reduce the peak velocity and decrease the diffusion to about 1.4 and would also increase the loading effectiveness to about 0.8. The peak velocities were supersonic at the higher exit velocity ratios. The modified blades could then operate at substantially higher exit velocities before supersonic velocities on the suction surfaces occurred.

Overall Performance

The overall performance of the blades is presented in terms of blade loading, total pressure loss, and kinetic energy loss for the range of ideal exit velocity ratios investigated.

Blade loading. - The change in the Zweifel blade loading coefficient with exit velocity is shown in figure 9(a). These values were calculated from the measured blade surface static pressures and are based on the calculated exit static pressure at station 3. The loading coefficients calculated from the tangential momentum, as determined from the exit surveys, were in close agreement with values shown in figure 9(a).

The loading coefficient decreases from 1.20 at the lowest exit velocity to 1.11 at the highest exit velocity. This trend was expected and was not necessarily the result of deterioration of blade performance. The actual blade pressure force increases with increasing velocity, but the ideal force increases more rapidly. This results in decreasing values of the loading coefficient with increasing exit velocity.

The change in the blade loading effectiveness parameter with exit velocity is shown in figure 9(b). The effectiveness parameter decreases about linearly from 0.782 at the lowest exit velocity to 0.698 at the highest exit velocity. The trend of the effectiveness parameter nearly parallels the trend of the Zweifel loading coefficient, which indicates

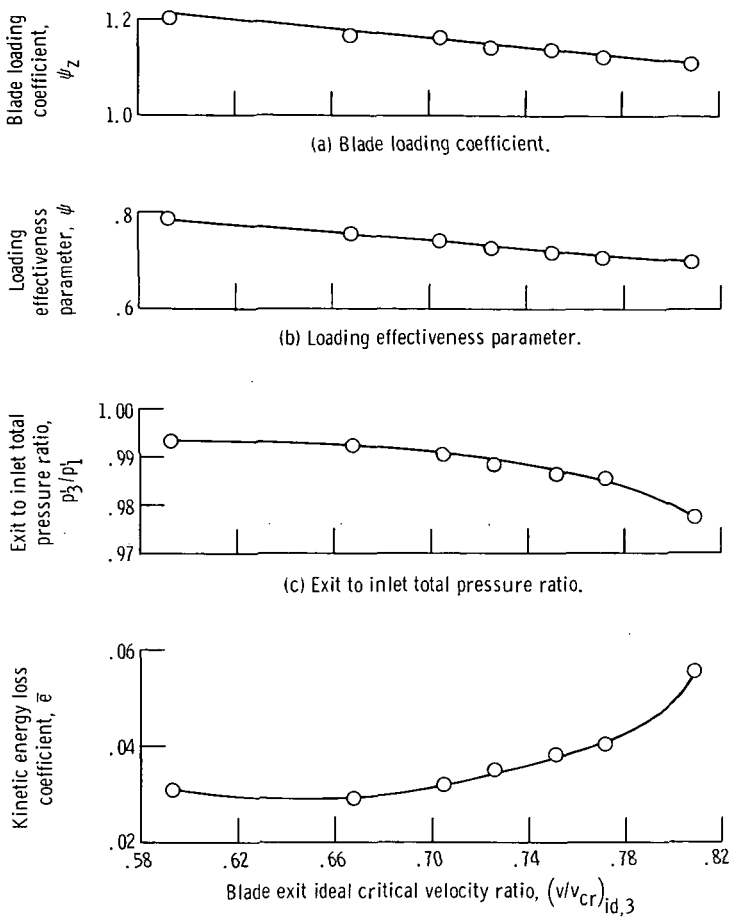

(a) Blade loading coefficient.

(b) Loading effectiveness parameter.

(c) Exit to inlet total pressure ratio.

(d) Kinetic energy loss coefficient.

Figure 9. - Overall performance.

that very little change occurred in the diffusion parameter over the range of exit velocities investigated.

Loss. - The variations of total pressure and kinetic energy loss with exit velocity are shown in figures 9(c) and (d), respectively. The ratio of exit to inlet total pressure decreases at an increasing rate as the ideal exit velocity ratio increases. This loss trend is reflected by the kinetic energy loss coefficient. The kinetic energy loss is almost constant up to an exit velocity ratio of 0.7. Then, there is a gradual increase in loss between exit velocity ratios of 0.7 and 0.77. At exit velocity ratios higher than 0.77, the loss increases rapidly. The trend of the kinetic energy loss with exit velocity is about the same as that indicated by the wake traces of figure 6.

The kinetic energy loss coefficient is correlated with the maximum blade suction surface velocities in figure 10. The rapid increase in loss begins just after the occurrence of supersonic velocities on the blade suction surface. The rapid increase in kinetic energy loss results from the additional total pressure loss that occurred at the

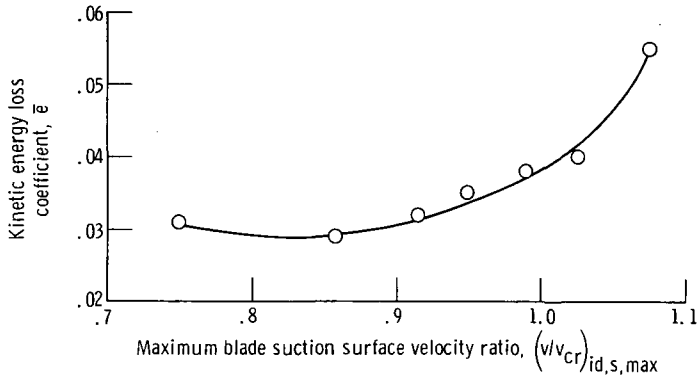

Figure 10. - Correlation of loss with maximum blade suction surface velocity.

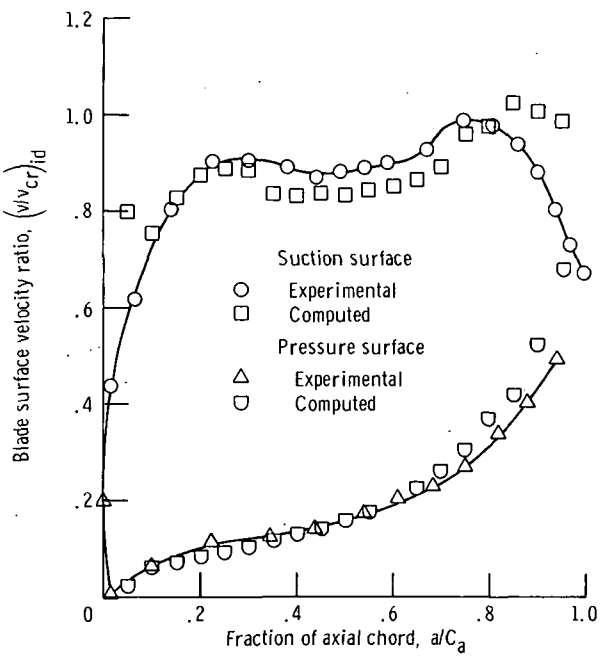

Figure 11. - Comparison of blade surface velocities determined from surface static-pressure measurements with computed velocities at ideal exit velocity ratio of 0.75.

higher exit velocity ratios. These additional losses were discussed in conjunction with the wake traces of figure 6. The additional pressure losses were probably influenced by the interaction of weak shocks, resulting from the supersonic velocities on the suction surface, with the boundary layer.

Comparison of Experimental and Analytical Results

In this section, the experimentally determined blade surface velocities and the cross-channel variation of velocity and flow angle are compared with the results obtained with the computer program of reference 9, which is for compressible flow with transonic velocities. The program input included the blade geometry, inlet and exit flow angles, and weight flow.

Blade surface velocities. - The blade surface velocity ratios from static-pressure measurements are compared with the computed values in figure 11. The curves are drawn through the experimental data. In general, there is very good agreement between the experimental and computed results. The only significant exception occurs on the suction surface near the trailing edge. Here, the computed velocities do not reflect the diffusion that occurred in this region.

Cross-channel velocity and angle. - The comparisons of the experimental and computed cross-channel variation of velocity and flow angle are shown in figures 12(a) and (b), respectively. The solid lines are the results of the blade exit survey at station 2. The dashed lines are the computed results at the same location. In the region between the blade wakes, the experimental and computed velocities are in very good agreement. The computed flow angle follows the trend of the measured flow angle very closely. The difference between the measured and computed angles in the region between the blade wakes is only about 2°. This difference between the measured and computed angles is probably due to the losses on the blade surfaces. These losses are not accounted for in the computer program.

The effect of the large cross-channel variation in pressures, velocity, and flow angle resulting from this very low-solidity stator on the performance of a succeeding blade row is not known. Because the flow conditions become more uniform farther downstream, one probable influence on performance would be the axial clearance between blade rows.

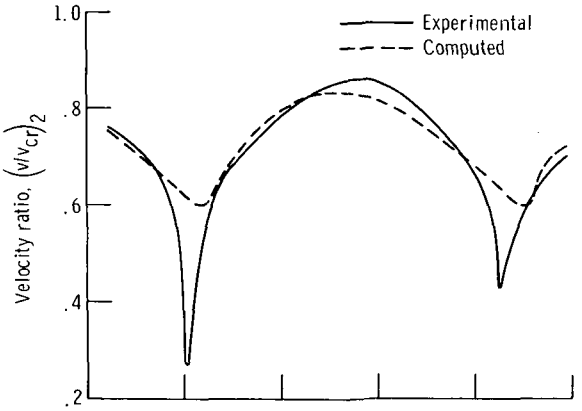

(a) Velocity.

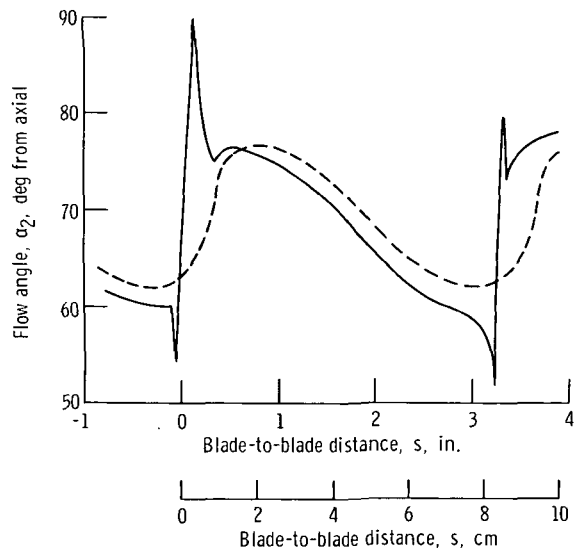

(b) Flow angle.

Figure 12. - Comparison of measured and computed blade-to-blade variation of velocity and flow angle at ideal exit velocity ratio of 0.75.

SUMMARY OF RESULTS

Very low-solidity blades were designed for a velocity diagram typical of the first stage of a jet engine turbine. The blade design criterion was high blade loading effectiveness. The performance of the blades was investigated experimentally in a simple two-dimensional cascade of six blades. The following results were obtained:

1. The flow apparently remained attached to the suction surfaces of the blades up to an ideal exit velocity ratio $(v/v_{cr})_{id,3}$ of about 0.7. At higher exit velocity ratios, separation began to occur. The separation and kinetic energy loss increased gradually up to an exit velocity ratio of about 0.77. At this point, separation and loss increased rapidly. At exit velocity ratios higher than 0.81, separation became severe. The rapid increase in separation and loss was correlated to the occurrence of supersonic velocities on the blade suction surfaces. The rapidly increasing separation and loss were probably incluenced by shock interaction with the boundary layer.

2. High blade loading effectiveness was achieved. At an exit velocity ratio of 0.75, the blade loading effectiveness was 0.715. However, a velocity peak occurred on the suction surface of the blade at about 75 percent of the axial chord. A modification of the suction surface to reduce these peak velocities would increase the blade loading effectiveness and delay the rapid increase in separation and loss to higher exit velocities.

3. The wide blade spacing and the high curvature and angles on the suction surface of the blade caused large variations in flow angle, static pressure, and weight flow across the channel in the plane of the trailing edge. The highest values of flow angle and static pressure and the lowest value of weight flow occurred near the suction surface of the blade.

4. The variation of velocity and flow angle across the channel in the plane of the trailing edge and the blade surface velocities was very close to the values predicted by a computer program similar to the one used in the design of the blades.

Lewis Research Center,
National Aeronautics and Space Administration,
Cleveland, Ohio, January 26, 1970,
720-03.

REFERENCES

1. Stewart, W. L.; and Glassman, A. J.: Advanced Concepts to Increase Turbine Blade Loading. Paper 68-WA/GT-11, ASME, Dec. 1968.

2. Nosek, Stanley M.; and Kline, John F.: Two-Dimensional Cascade Investigation of a Turbine Tandem Blade Design. NASA TM X-1836, 1969.

3. Lueders, H. G.; and Roelke, R. J.: Some Experimental Results of Two Concepts Designed to Increase Turbine Blade Loading. Paper 69-WA/GT-1, ASME, Nov. 1969.

4. Bettner, James L.; and Nosek, Stanley M.: Summary of Tests on Two Highly Loaded Turbine Blade Concepts in Three-Dimensional Cascade Sector. Paper 69-WA/GT, ASME, Nov. 1969.

5. Whitney, Warren J.; Szanca, Edward M.; Moffitt, Thomas P.; and Monroe, Daniel E.: Cold-Air Investigation of a Turbine For High-Temperature-Engine Application. I. Turbine Design and Overall Stator Performance. NASA TN D-3751, 1967.

6. Zweifel, O.: The Spacing of Turbo-Machine Blading, Especially With Large Angular Deflection. Brown Boveri Rev. vol. 32, no. 12, Dec. 1945, pp. 436-444.

7. Miser, James W.; Stewart, Warner L.; and Whitney, Warren J.: Analysis of Turbomachine Viscous Losses Affected by Changes in Blade Geometry. NACA RM E56F21, 1956.

8. Katsanis, Theodore: A Computer Program for Calculating Velocities and Streamlines for Two-Dimensional, Incompressible Flow in Axial Blade Rows. NASA TN D-3762, 1967.

9. Katsanis, Theodore: Fortran Program for Calculating Transonic Velocities on a Blade-to-Blade Stream Surface of a Turbomachine. NASA TN D-5427, 1969.

NASA-Langley, 1970 — 1 E-5490

NATIONAL AERONAUTICS AND SPACE ADMINISTRATION
WASHINGTON, D.C. 20546

OFFICIAL BUSINESS

FIRST CLASS MAIL

POSTAGE AND FEES PAID
NATIONAL AERONAUTICS AND
SPACE ADMINISTRATION

POSTMASTER: If Undeliverable (Section 158 Postal Manual) Do Not Return

"The aeronautical and space activities of the United States shall be conducted so as to contribute . . . to the expansion of human knowledge of phenomena in the atmosphere and space. The Administration shall provide for the widest practicable and appropriate dissemination of information concerning its activities and the results thereof."

—NATIONAL AERONAUTICS AND SPACE ACT OF 1958

NASA SCIENTIFIC AND TECHNICAL PUBLICATIONS

TECHNICAL REPORTS: Scientific and technical information considered important, complete, and a lasting contribution to existing knowledge.

TECHNICAL NOTES: Information less broad in scope but nevertheless of importance as a contribution to existing knowledge.

TECHNICAL MEMORANDUMS: Information receiving limited distribution because of preliminary data, security classification, or other reasons.

CONTRACTOR REPORTS: Scientific and technical information generated under a NASA contract or grant and considered an important contribution to existing knowledge.

TECHNICAL TRANSLATIONS: Information published in a foreign language considered to merit NASA distribution in English.

SPECIAL PUBLICATIONS: Information derived from or of value to NASA activities. Publications include conference proceedings, monographs, data compilations, handbooks, sourcebooks, and special bibliographies.

TECHNOLOGY UTILIZATION PUBLICATIONS: Information on technology used by NASA that may be of particular interest in commercial and other non-aerospace applications. Publications include Tech Briefs, Technology Utilization Reports and Notes, and Technology Surveys.

Details on the availability of these publications may be obtained from:

SCIENTIFIC AND TECHNICAL INFORMATION DIVISION

NATIONAL AERONAUTICS AND SPACE ADMINISTRATION

Washington, D.C. 20546